JOURNAL OF MATERIALS SCIENCE: MATERIALS IN MEDICINE 11 (2000) 49–60

Bending and fracture of compact circumferential and osteonal lamellar bone of the baboon tibia

D. LIU, H. D. WAGNER*, S. WEINER‡
Departments of Structural Biology and Materials and Interfaces, Weizmann Institute of Science, Rehovot, Israel 76100*

Lamellar bone is common among primates, either in the form of extended planar circumferential arrays, or as cylindrically shaped osteons. Osteonal bone generally replaces circumferential lamellar bone with time, and it is therefore of much interest to compare the mechanical properties and fracture behavior of these two forms of lamellar bone. This is, however, difficult as natural specimens of circumferential lamellar bone large enough for standard mechanical tests are not available. We found that as a result of treatment with large doses of alendronate, the lateral sides of the diaphyses of baboon tibia contained fairly extensive regions of circumferential lamellar bone, the structure of which appears to be indistinguishable from untreated lamellar bone. Three-point bending tests were used to determine the elastic and ultimate properties of almost pure circumferential lamellar bone and osteonal bone in four different orientations relative to the tibia long axis. After taking into account the differences in porosity and extent of mineralization of the two bone types, the flexural modulus, bending strength, fracture strain and nominal work-to-fracture properties were similar for the same orientations, with some exceptions. This implies that it is the lamellar structure itself that is mainly responsible for these mechanical properties. The fracture behavior and morphologies of the fracture surfaces varied significantly with orientation in both types of bone. This is related to the microstructure of lamellar bone. Osteonal bone exhibited quite different damage-related behavior during fracture as compared to circumferential lamellar bone. Following fracture the two halves of osteonal bone remained attached whereas in circumferential lamellar bone they separated. These differences could well provide significant adaptive advantages to osteonal bone function.

1. Introduction

The family of mineralized collagen-based biological materials fulfill a wide variety of functions in vertebrates. This family includes the various bone and dentin types, cementum and mineralized tendons. Each of these materials has a different structure that, in some way, presumably reflects the function it performs. Much effort has been expended on understanding the relations between structure and function [1], but there are still wide gaps in our knowledge.

Lamellar bone is widely distributed, particularly among mammals, and is the most common bone type in primates [2, 3]. It has therefore been the subject of intensive study, both with respect to structure and mechanical properties. It is also perhaps the most complex of all the bone types in terms of structure, and this has made the study of its structure–mechanical relations particularly difficult. The following is a very brief overview of the structure of lamellar bone.

The collagen fibril with its layers of plate-shaped crystals of carbonated apatite is regarded as the basic building block [4–7]. These mineralized fibrils are arranged in lamellae. Each lamella is composed of aligned mineralized fibrils and in subsequent lamellae the orientations of the fibrils change, to form a plywood-like structure [8–11]. Some investigators perceive the structure as being composed of alternating layers of collagen-rich and collagen-poor material with an interwoven arrangement of fibers [12, 13]. At a higher level of organization, the initially deposited primary lamellae can be organized in extended planar arrays, which in the primates are in a circumferential plane about the central marrow cavity [2]. We therefore refer to this bone type as circumferential lamellar bone (CLB). When internal remodeling occurs, the secondary bone that replaces the primarily formed bone is also lamellar bone, but is in the form of cylinders. These are known as Haversian systems or secondary osteons. This osteonal bone (OB) with its usually minor amount of interstitial primary CLB bone remaining between osteons, is the major component of mature compact bone in primates.

This already complex structure is further complicated

‡Author to whom correspondence should be addressed.

by several important age-related variables. The amount of mineral present in a given parcel of solid bone increases relative to the other major components, collagen and water, with time [14]. This additional mineral forms within the fibrils and possibly between fibrils [15]. Porosity is the second variable that changes with age and between different bone types [16, 17], and the extent of internal osteonal remodeling is the third [18]. In addition, the proportions of differently oriented mineralized collagen fibrils within the osteons can vary locally in a given bone, apparently as a function of the nature of the prevailing stress field [19–22].

The bulk mechanical properties of compact lamellar bone are well known [1]. As most mechanical tests require macroscopic specimens (for bending tests ten or more millimeters in length and a span-thickness ratio of 7:15 is required [16, 23]), almost all information on pure lamellar bone relates to osteonal bone from relatively large animals. Note that bovine bone prior to being remodeled is a mixture of lamellar bone, and bone comprising arrays of aligned mineralized collagen fibers (parallel fibered bone) [3]. One exception is the study of single osteons [24], which shows a direct relation between osteonal lamellar structure in terms of mineralized collagen orientation and mechanical properties. A second exception is the studies using microhardness, which has been used, for example, to investigate the lamellar structure of circumferential lamellar bone in different orientations [25]. Microhardness values, however, are difficult to relate to the inherent elastic and ultimate properties, and hence only general trends can be obtained. Thus to date it is not possible to discriminate between the contribution of the lamellar structure itself to the bulk mechanical properties, and the contribution of the lamellae in the form of osteons. Many investigators have noted that secondary osteonal bone is weaker than primary bone [26, 27], but in all these studies the primary bone referred to is not primary circumferential lamellar bone, but primary fibrolamellar bone (also known as plexiform), which is a mixture of parallel fibered bone and lamellar bone [3].

In this study we take advantage of the fact that the medial sides of the diaphyses of several baboon tibiae that were used in the initial studies of the effect of the bisphosphonate, alendronate, on remodeling [28, 29] contain fairly extensive areas of CLB. Alendronate affects the activities of cells that remove bone (osteoclasts) [28, 29]. This presumably came about because these animals began receiving the alendronate at about the same time as remodeling ensued in this part of the bone. The untreated control animals contained many more osteons (about 30%) at this location. The presence of this extensive CLB thus afforded us a unique opportunity to compare planar arrays of lamellar bone almost devoid of osteons, with bone that is almost entirely (greater than 90%) osteonal.

This comparison is based on the assumption that the lamellar structure of the bones from alendronate-treated animals is the same as in the untreated control animals. As alendronate affects the remodeling process, differences in bone mineral content and porosity do exist and are taken into account in the analysis of the results. Mechanical tests indicate that the ''quality'' of bone that accreted after alendronate treatment showed no deleterious effects [29]. This indirect observation suggests that if structural differences do exist they are probably minor. Direct comparisons of the lamellae themselves at the histological level on polished bone surfaces (Fig. 1), and in particular of fracture surfaces using the scanning electron microscope (SEM; Fig. 2) show no consistent differences. Although these observations do not constitute a complete structural analysis of these bones at all hierarchical levels, we think it is reasonable to assume that up to the lamellar level the structures of the two bones being compared are essentially the same.

We used a three-point bending test, as the maximum available specimen size was limited to about 15 mm in the longest direction, and we were particularly interested in the modes of bone fracture, which in nature are often produced by bending stresses. This test has some drawbacks as it involves tensile, compressive and shearing stresses [23]. Another drawback is the application of linear elastic theory to calculate the bending strength and strain, as the post-yield deformation will increase the calculated strength [30]. We chose to study the bone specimens in four orientations relative to the tibia long axis, as this provides both insight into the dependence of orientation on mechanical function, and a comprehensive set of data that can, in the future, be modeled mathematically to clarify structure–function relations further. Here we show that in general the elastic and ultimate properties of both the OB and CLB specimens studied are dominated by the lamellar structure itself, but the localized organization of the lamellae into the many cylinders that constitute the bulk of osteonal bone, affords some important benefits, particularly during fracture.

2. Materials and methods

2.1. Materials

Four left tibia of two groups of frozen adult female baboons (*Papio anubis*) were used in this test. One group was untreated, whereas a second group was ovariectomized and then received 0.05 mg kg^{-1} intravenously (i.v.) alendronate every two weeks for two years. For more details of the experimental protocol and the results of the studies of these bones, see Thompson *et al.* [28] and Balena *et al.* [29]. Three centimeter diaphyseal sections were dissected 4.5 cm below the tibial tuberosity. The samples were kept frozen until use. Transverse sections of several millimeters thick were cut, embedded in methylmethacrylate (Buehler Ultra-mount) and ground and polished (Buehler Minimet Polisher) using 320, 400 and 600 grit grinding papers, followed by 6 and 1 μm diamond pastes, and finally 0.05 μm aluminum paste. They were examined by light microscopy (Leitz Metallux 3). Areas of secondary osteonal and primary circumferential lamellar bone were evident (Fig. 1). In the alendronate-treated bones the medial side was composed almost entirely of CLB with only a few secondary osteons close to the endosteal surface (Fig. 1a). Osteonal samples were obtained from the lateral side of control bones (Fig. 1b) after removal of the circumferential lamellar areas adjacent to the bone surface. We were obliged to use the lateral side of the

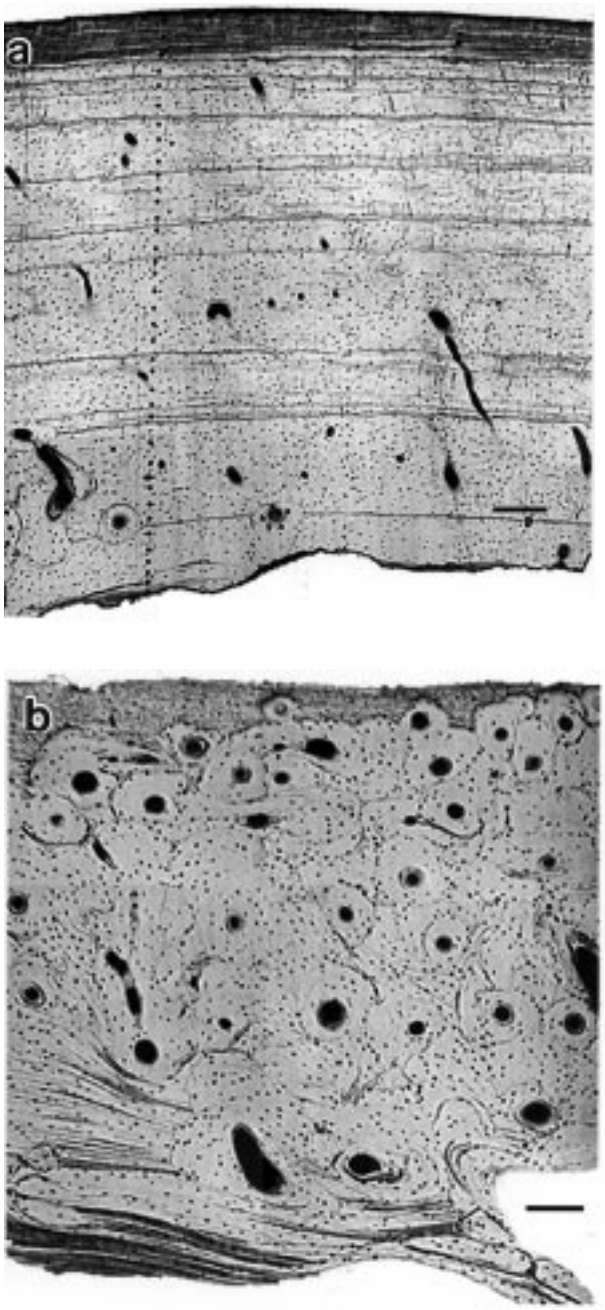

Figure 1 Light microscope photographs of the polished surfaces of baboon tibiae in transverse section: (a) Circumferential lamellar bone (CLB) is predominant from the periosteal surface (top) to the endosteal surface (bottom) in the medial side of alendronate-treated bone. The line of black dots is due to microhardness indentations. (b) Osteonal bone is predominant in the central portion of the lateral side of control tibiae. Localized areas of CLB are present close to the periosteal and endosteal surfaces. These were removed mechanically prior to testing (scale bars: 0.25 mm).

diaphysis of the control and the medial side of the alendronate-treated baboon, because the medial side of the control and the lateral side of the alendronate-treated tibia are mixtures of CLB and OB structures. In the human femur, small but significant differences in elastic properties do exist in opposing segments of the diaphysis [31], but these differences were not detected in fracture [32].

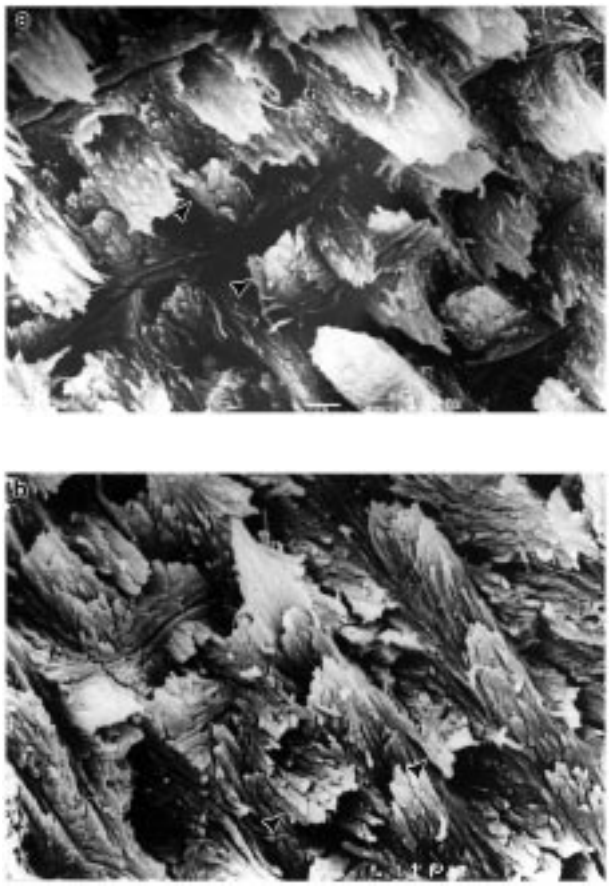

Figure 2 SEM micrographs of the fracture surface of a circumferential lamellar (a) and an osteonal (b) type A bending specimen at 90° showing the lamellar structure and prominent ''back-flip'' sublamella, following Weiner *et al*. [11] (arrowheads), as well as the pull-out features that leave holes in the surface.

2.2. Sample preparation for three-point bending tests

Rectangular shaped samples ($1.0 \times 1.0 \times 15.0$ mm) were machined using a low-speed water-cooled diamond saw (South Bay Technology Inc.) modified by the addition of a 360° rotating sample holder. The samples were oriented with respect to the bone long axis (Fig. 3a and b) using the co-ordinate system of Reilly and Burstein [33] (Fig. 3a), namely the x-axis is parallel to the bone long axis, the y-axis is in the tangential direction and the z-axis in the radial direction. Samples were cut from one tibia in four different orientations in the x–y plane (Fig. 3b), with the long axis of the samples defining angles of 0, 30, 60 and 90° with the x-axis. Between three and five specimens were tested in each orientation except for one group (see Table I) where only two specimens were available. The numbers of specimens of each bone type tested for reproducibility were limited by the size of the tibia diaphysis, as all the specimens in four different orientations were extracted from one tibia. The samples from one particular bone type, were termed a ''set''. One set of CLB, and one set of OB were prepared for bending with the load direction perpendicular to the periosteal surface (bending mode type A, Fig. 3c). A third set of CLB was tested in bending mode type B (Fig. 3d). In addition a group of osteonal bones cut at 0 and 90° was prepared with V-type notches using a saw-tooth edge solid carbide circular blade for work-to-fracture

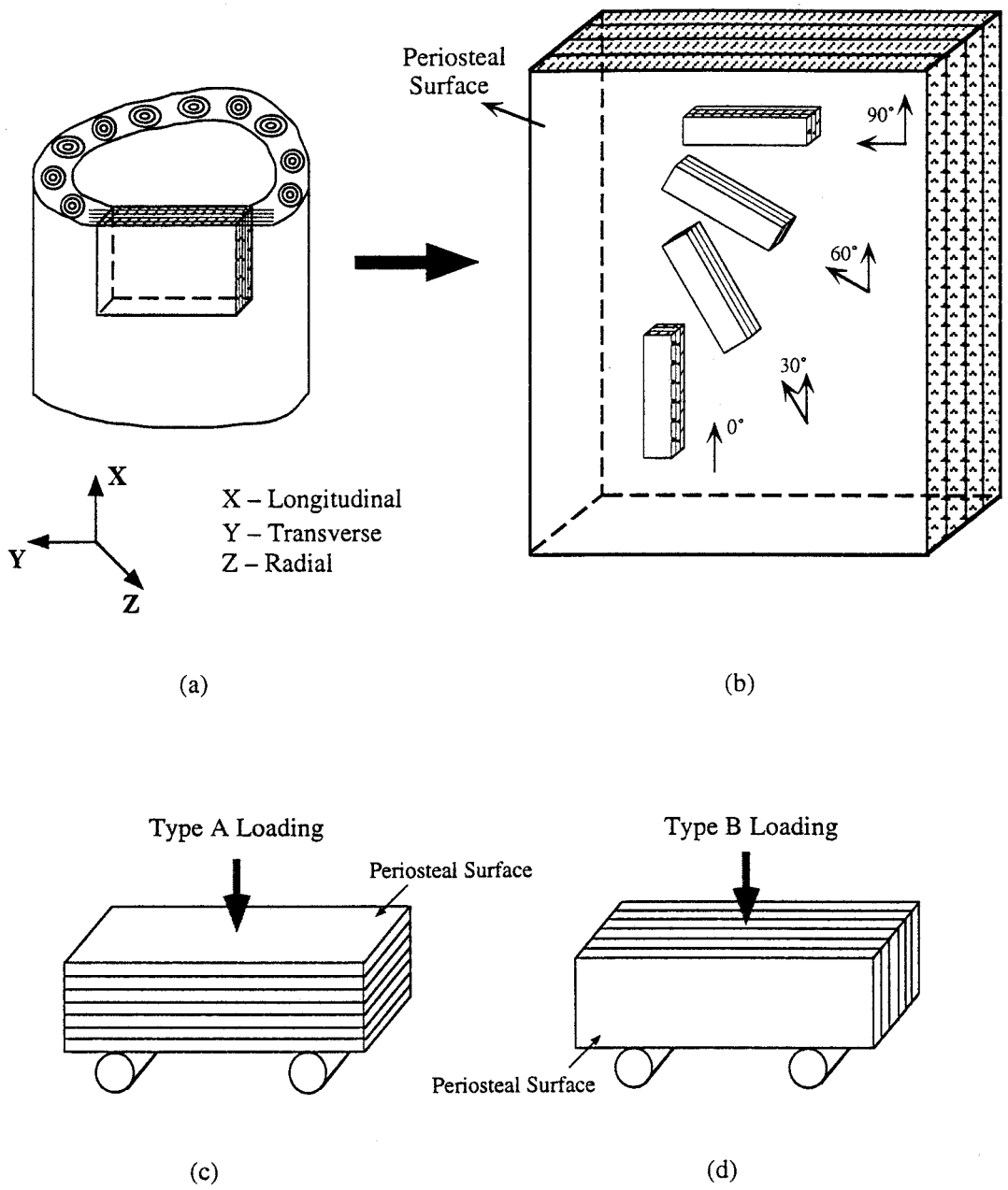

Figure 3 Schematic diagrams showing the sampling locations and orientations of the circumferential lamellar bone specimens. Note that the schemes shown in (a) and (b) also apply to the osteonal bone specimens, except that they were obtained from the lateral side of the midshaft. (a) Sample location and axial frame of reference follow Reilly and Burstein [33]. (b) The four orientations of the specimens that comprise one set. (c) The type A bending direction and (d) the type B bending direction of CLB specimens.

measurements using bending type A. The ratio of notch length : sample depth was 1 : 3. Four baboon tibiae were used, and the total number of specimens tested was 54.

2.3. Bending test

An Instron model 4502 was used for the measurement of mechanical properties. The test span was 9 mm, as limited by the shortest sample length (15 mm) available. The choice of the loading rate (0.5 mm min^{-1}) was based on previous studies [17, 23] and the fact that the size of the samples used was very small. The surfaces of the samples were dried with a tissue just before the bending test. Each test lasted about 2 min.

From each load–displacement curve, flexural modulus, bending strength, fracture strain and nominal work-to-fracture were calculated. The flexural modulus, E (GPa), stress, β (MPa), and strain, (m m^{-1}), were computed using the following formulae

$$E = FL^3/(4\partial ba^3) \quad (1)$$

$$\beta = 3FL/(2ba^2) \quad (2)$$

$$= 6\partial a/L^2 \quad (3)$$

where F (N) is the load, L (m) is the span of the bending test, b (m) is the specimen width, a (m) is the specimen height, and, ∂ (m) is the displacement. Fracture strain is the ultimate strain for CLB specimens. For OB specimens fracture strain was calculated from the greatest

TABLE I Mean, standard deviation (in parentheses) and number of specimens (in brackets)[a] of the bending tests of circumferential lamellar and osteonal bone

		Circumferential lamellar bone		Osteonal bone	t-test[c]
		Type[b] A	Type B	Type A	
Flexural modulus, GPa	0°	15.5(4.83) [3]	14.6(1.17) [3]	14.4(1.18) [5]	$p > 0.05$
	30°	14.3(2.60) [3]	13.6(1.10) [3]	10.7(0.94) [4]	$p < 0.05$[e]
	60°	10.0(0.37) [4]	10.6(0.63) [3]	8.1(0.73) [2]	$p < 0.05$[e]
	90°	8.6(0.36) [3]	8.8(0.64) [3]	7.6(0.79) [5]	$p > 0.05$
Bending strength, MPa	0°	350(32.7)	309(19.0)	289(21.6)	$p < 0.02$[e]
	30°	194(42.6)	225(55.5)	130(18.2)	$p < 0.02$[e]
	60°	120(13.1)	148(12.5)	71(4.8)	$p < 0.05$[e]
	90°	104(10.6)	109(11.3)	71(10.5)	$p < 0.005$[e]
Fracture strain, %	0°	7.1(1.42)	4.8(1.44)	6.0(1.36)	$p > 0.1$
	30°	2.9(1.46)	2.3(0.55)	2.1(0.46)	$p > 0.1$
	60°	1.4(0.32)	1.8(0.12)	1.4(0.01)	$p > 0.5$
	90°	1.3(0.36)	1.5(0.17)	1.6(0.31)	$p > 0.1$
Nominal work-to-fracture[d], kJ m^{-2}	0°	7.76(1.45)	5.34(2.39)	7.12(1.89)	$p > 0.5$
	30°	2.43(0.60)	1.74(0.39)	0.88(0.25)	$p < 0.01$[e]
	60°	0.48(0.08)	0.73(0.08)	0.40(0.01)	$p > 0.2$
	90°	0.34(0.10)	0.44(0.07)	0.40(0.11)	$p > 0.2$

[a] Number of specimens tested applies to all bending parameters.
[b] The bending types are shown in Fig. 2.
[c] T-test results are for mechanical properties of CLB and OB specimens of bending type A only.
[d] The nominal work-to-fracture from notched specimens of the control baboon tibia are 2.76(0.29) [4] and 0.39(0.03) [3] kJ m^{-2} for the 0 and 90° orientations, respectively; while those for unnotched specimens from the same tibia are 3.76(0.81) [3] and 0.38(0.04) [3] kJ m^{-2} for the 0 and 90° orientations.
[e] Data that show significant difference.

decrease in load until an arbitrary threshold of 1 N. This is where the greatest change in the slope of the curve occurs after the ultimate load point. The nominal work-to-fracture was calculated by dividing the area under the load–displacement curve by twice the nominal cross-sectional area of the specimen. This measurement differs from the real work-to-fracture in two respects: the arbitrary unit area of the fracture surface used in the calculation is the ideally flat cross-section of the specimen irrespective of the actual fracture path, and the specimens were not notched because of the necessity for using relatively small specimens in this study. The former assumption increases the calculated values of the 0° and to some extent the 30° specimens, because indeed they did have an undulating fracture path, but on the other hand highlights this important aspect of the fracture behavior. The significance of notching was tested by comparing notched and unnotched specimens in the 0 and 90° orientations. In the 0° orientation, the notched specimens produced lower values (the calculation did not include the area of the notch) than the unnotched specimens, much smoother fracture surfaces and fewer steps. No difference was observed in the 90° orientation (Table I).

2.4. Scanning electron microscope (SEM) examination of the fracture surface

One-half of the fractured specimen was dried and cut a few millimeters below the fracture surface. It was attached with double-sided carbon tape to an aluminum stub, coated with gold and examined in a Jeol 6400 SEM. The texture of the fracture surface was examined.

2.5. Light microscope examination of the fracture profile

The wet second-half of the fractured specimen was embedded and polished as described above. After the bending test, the samples were photographed through a Leica Wild M8 binocular with a scanning CCD camera (Microlumina, Leaf Systems). The porosities of the CLB and OB specimens were measured from photographs (taken by Leitz Metallux 3) of polished surfaces at a magnification of × 50. The proportions of bone material and pores were calculated using NIH Image, after setting a threshold value such that the pores were displayed black and the bone white. The areas adjacent to the fracture surfaces of the bending specimens (0 and 90°) were analyzed. The Haversian canals and osteocytes were included.

2.6. Ash weight

Weighed aliquots of powdered bone were heated in an oven at 550 °C until a constant weight was obtained (usually 24 h), and then reweighed.

2.7. Microhardness

Microhardness was measured on the moist polished specimens using a Leitz microhardness tester attached to a light microscope (Leitz Metallux 3) equipped with a video imaging system (Aplitec MSV-800). Vickers indents were produced using a force of 0.245 N (as calibrated by the manufacturer) for 15 s. The samples were kept moist during the test.

3. Results

The CLB specimens were composed mostly of lamellae parallel to the endosteal and periosteal surfaces, with secondary osteons comprising only a small volume of the bone in the endosteal region (Fig. 1a). The OB specimens (after mechanical removal of the periosteal and endosteal circumferential lamellar portions) were composed mostly of cylindrically shaped secondary osteons with the small spaces between them comprising primary lamellar bone (Fig. 1b). Thus both the CLB and OB specimens were composed entirely of lamellar bone, with the former being mostly primary lamellar bone in the form of extended planar lamellae, and the latter mostly secondary lamellar bone in the form of osteons.

These differences are reflected in the hardness values. The hardness of the primary bone was greater than that of the secondary bone (Table II). Note also that the hardness of the primary circumferential lamellar bone between the osteons of the OB specimens was significantly less than the primary circumferential lamellar bone of the CLB specimens. This may reflect the fact that the latter was older than the former, due to the treatment with alendronate. It may also be due to the OB and CLB specimens being derived from the medial and lateral parts of the mid-shaft of the diaphysis, respectively. Table II also shows that the ash weights of the CLB specimens were considerably greater than those of the OB specimens, reflecting the hardness value differences and in turn the varying proportions of primary and secondary lamellar bone. The porosity of the OB bone was more than three times that of the CLB bone.

Fig. 4 shows typical stress–strain curves obtained from the three-point bending tests of CLB and OB specimens in four orientations (Fig. 3) with bending type A. The mechanical properties of both the CLB and OB specimens varied significantly with orientation in the longitudinal–transverse plane. A qualitative comparison of these CLB and OB specimen stress–strain curves revealed some interesting differences (Fig. 4). Of particular interest were the prominence of features characteristic of significant damage-related phenomena [34] in the OB specimens, and the ''tails'', which show that the OB bones do not fracture as cleanly as the CLB bones.

Table I lists the calculated means, standard deviations and the *t*-test results of the elastic and ultimate properties of the specimen sets and a comparison of the work-to-fracture measurements of the notched specimens with the unnotched specimens that were used to calculate the nominal work-to-fracture. The dependence of all four

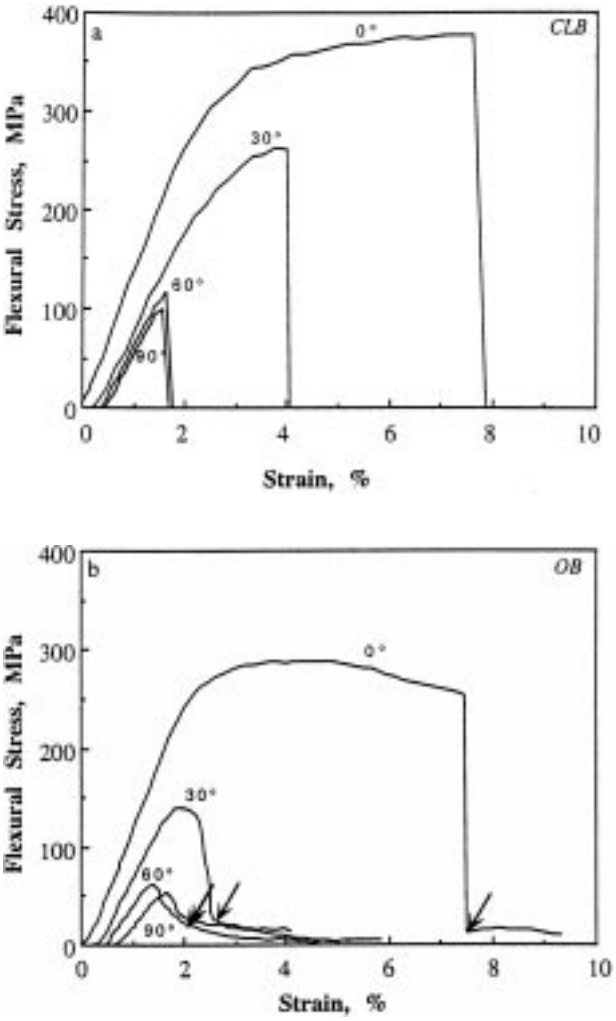

Figure 4 Flexural stress–strain curves of typical (a) circumferential lamellar bone specimens and (b) osteonal bone specimens in different orientations with respect to the bone long axis with bending type A. Arrows show the points used for the measurement of fracture strain.

mechanical properties on specimen orientation is very prominent. This is consistent with modulus and strength measurements made on bovine and human bone by, for example, Dempster and Liddicoat [35], Reilly and Burstein [33], Bonfield and Grynpas [36] and Katz [37]. Fig. 5 graphically compares the results of the CLB specimens tested in the type A orientation with the OB specimens. In the CLB type A orientation the stress was exerted on planes parallel to the natural bone surface. As this was also the case for the OB specimens, it is most appropriate to compare these two sets of data directly. They both show a strong dependence on sample orientation and have similar trends for all four

TABLE II Mean, standard deviation and *t*-test results of hardness, ash weights and porosities of control and alendronate-treated baboon tibiae

	Control	Alendronate-treated	*t*-test
Hardness of CLB, kg mm^{-2} [a]	65($\pm$4.5)	75($\pm$2.3)	$p<0.01$
Hardness range of OB, kg mm^{-2} [b]	30–70	25–70	
Ash weights,%	66($\pm$0.4)	69($\pm$0.3)	$p<0.005$[c]
Porosity,% [d]	7.4($\pm$2.9)	2.2($\pm$0.92)	$p<0.01$

[a] 1 kg mm^{-2} = 9.81 MPa.
[b] The wide range of hardness values results from the variability in the degree of mineralization.
[c] $p<0.005$ means that the probability that it is incorrect to state that the two means are different is less than 0.005.
[d] Porosity of the area for bending tests.

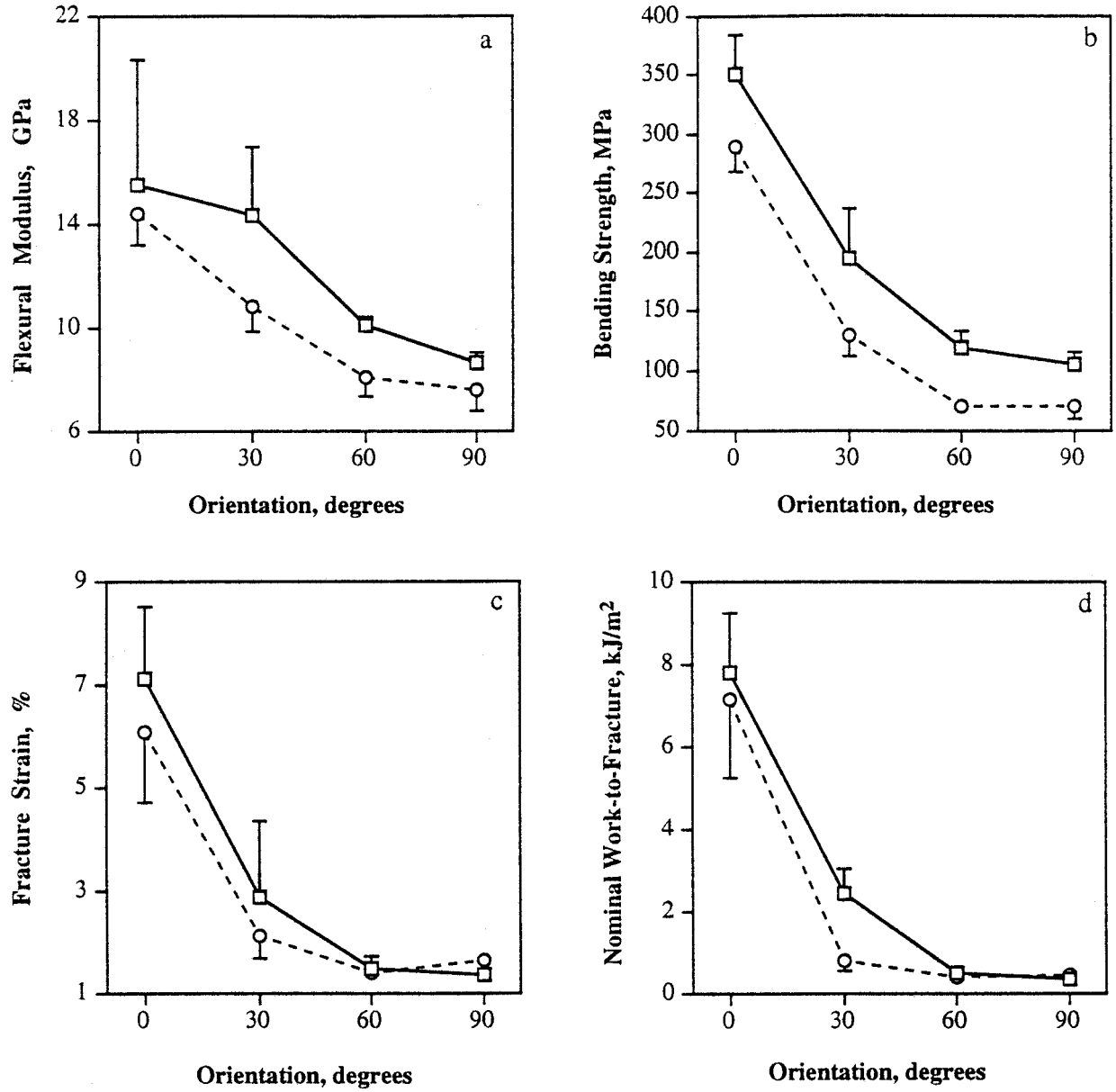

Figure 5 Three-point bending results as a function of orientation with respect to the long axis of circumferential lamellar bone type A (—□—) and osteonal (- -○- -) specimens. Data are from Table I.

mechanical properties measured. The curves of the flexural modulus and bending strength are clearly offset from each other. The *t*-test results show that the flexural modulus is different for the 30 and 60° orientations. The bending strengths in all four orientations of CLB are higher than those of OB specimens. The absolute values obtained from the CLB and OB specimens for the fracture strain and the nominal work-to-fracture are the same, except for the 30° orientation measurements for the nominal work-to-fracture, which are significantly different.

Examination of the fracture surfaces of the broken CLB and OB specimens revealed consistent and clear-cut differences as a function of orientation. The fracture surfaces of the 90 and 60° specimens were almost flat, whereas the 30° and in particular the 0° specimens, were undulating (Figs 6 and 7). This undulation is particularly apparent when the sections are viewed edge-on in the light microscope (Fig. 6). Additional cracks can also be seen on the tensile side of the specimens in the 0° orientation. In the OB specimens oriented at 0°, there are local areas where the crack follows the osteon boundaries (*i.e.* the cement lines), but for the most part, the crack pathway is either roughly perpendicular to, or parallel to the periosteal and endosteal surfaces. At higher magnifications, as viewed in the SEM, the 0° oriented CLB and OB specimens have a ceramic-like texture, whereas the 90° oriented specimens show very clearly the lamellar structure (Fig. 8). We also noted that after fracture was complete, the CLB specimens inevitably broke into two unconnected pieces, whereas the OB specimens remained attached to each other. An example of the latter is shown in Fig. 9.

The extent to which these bones are anisotropic, varies considerably. For convenience, Table III shows the ratios of the values at 0 and 90°, which follow Turner *et al.* [39], we refer to as the anisotropy ratio. Note that the anisotropy ratios of the work-to-fracture are about ten times greater than those of the flexural modulus.

The comparison of the bending results of the CLB specimens in the type A and type B orientations, which are rotated 90° with respect to the lamellar boundary

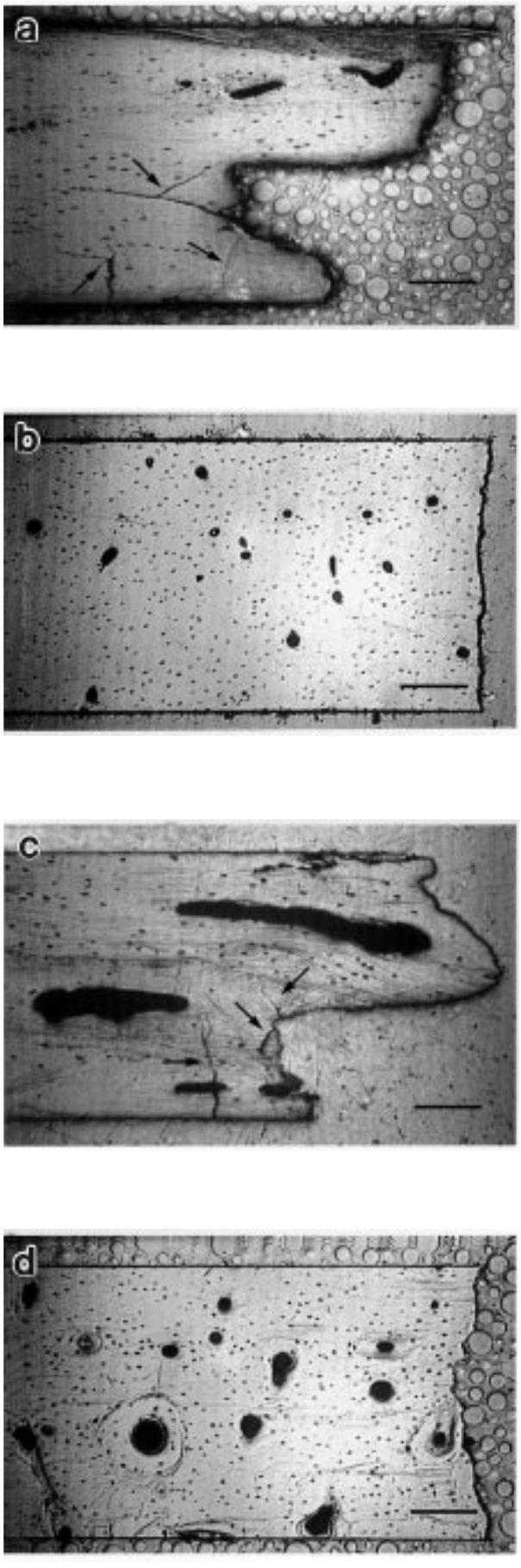

Figure 6 Light microscope photographs of the polished surfaces viewed edge-on to the fracture planes (right-hand side) of CLB specimens at 0° (a) and 90° (b), as well as OB specimens at 0° (c) and 90° (d). The tension sides of the specimens are at the bottom of each photograph, and the arrows show the locations of prominent cracks (scale bars: 0.5 mm).

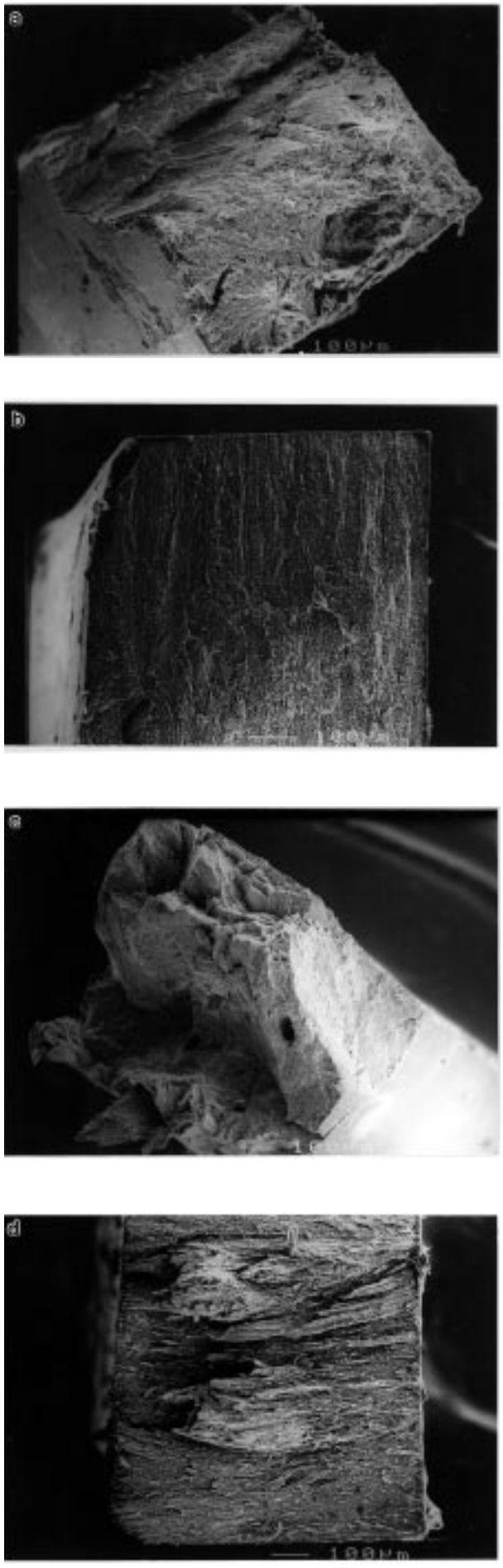

Figure 7 SEM micrographs of representative fracture surfaces of type A circumferential lamellar bone specimens at 0° (a) and 90° (b), and osteonal bone specimens at 0° (c) and 90° (d).

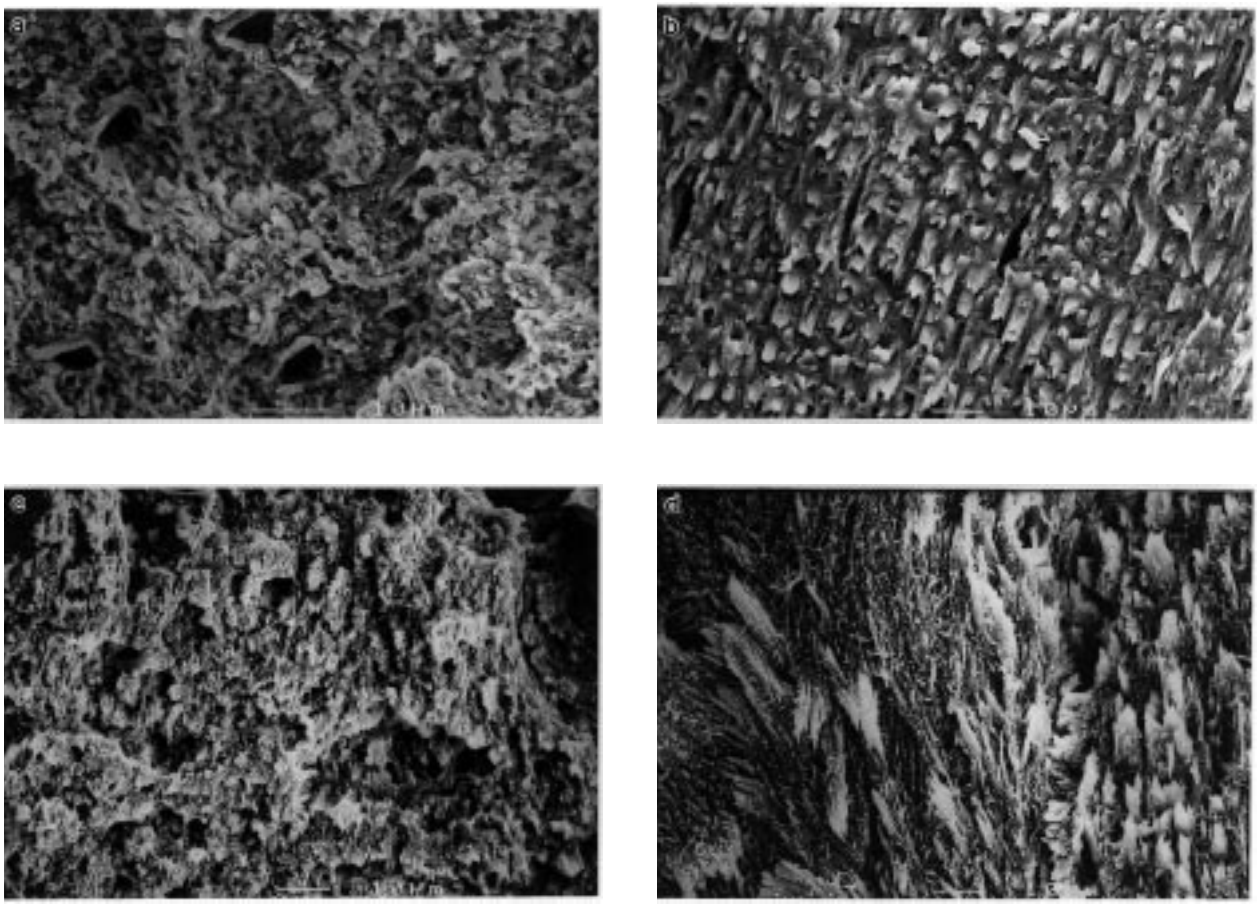

Figure 8 SEM micrographs of the fracture surfaces of circumferential lamellar bone specimens in type A bending at 0° (a) and 90° (b), and osteonal bone specimens at 0° (c) and 90° (d). Note that the 0° fracture surfaces shown are in the *y–z* plane and the 90° surfaces are in the *x–z* plane. Note too that in (d) the lamellar structure is viewed in different orientations as this is a section through part of an osteon. The fracture surface in (d) is also more fibrous than in (b), probably as a result of the fact that the osteonal bone is less mineralized than the circumferential lamellar bone [38].

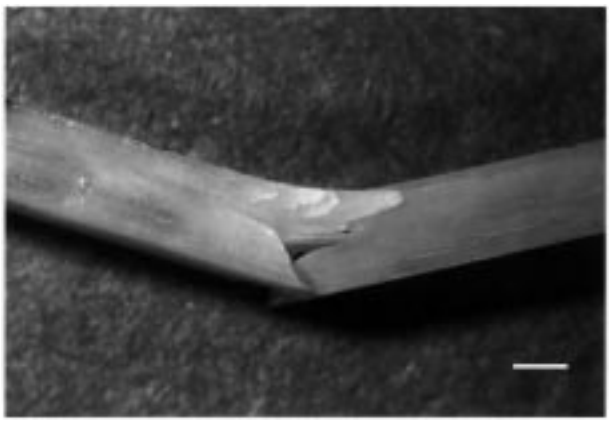

Figure 9 Light microscope photograph of osteonal bone (0°) after fracture in three-point bending, showing the two halves of the bone still attached to each other (scale bar: 0.5 mm).

TABLE III Ratios of mechanical properties[a] between longitudinal and transverse specimens

	$E_{0°}/E_{90°}$	$\sigma_{b0°}/\sigma_{b90°}$	$\varepsilon_{f0°}/\varepsilon_{f90°}$	$W_{0°}/W_{90°}$
CLB, type A	1.8	3.4	5.3	22.2
CLB, type B	1.7	2.8	3.2	12.2
OB, type A	1.9	4.1	3.7	17.7

[a] E, flexural modulus; σ_b, bending strength; ε_f, fracture strain; W, nominal work-to-fracture. Subscripts represent the orientation of the specimens.

planes, revealed no significant differences for the flexural modulus. Some significant differences were observed, however, in the bending strength at 0 and 90°, fracture strain and nominal work-to-fracture measurements at 60°.

4. Discussion

A comparison of the elastic and ultimate properties of compact circumferential lamellar bone and compact osteonal bone from the baboon tibia, showed for the most part, remarkable similarities. Both bone types exhibited a strong anisotropic dependence on sample orientation with respect to the long axis of the bone. This implies that it is the complex arrangement of the mineralized collagen fibrils that constitutes most of this structure, that is mainly responsible for the mechanical properties of lamellar bone. The most significant differences related to certain aspects of the fracture behavior. These can be mostly ascribed to the contribution of the secondary osteons to bone bulk properties.

The flexural modulus measurements of CLB and OB bones showed that the overall general trend with varying specimen orientation is similar, but the curves are offset. Furthermore, the extent of the offset varies, with the largest value being for the 30° orientation (Table I, Fig. 5). Thus the organization of the lamellae into small cylinders (osteons) rather than planar extended sheets (circumferential lamellae) did apparently influence the

modulus values to some extent, particularly at the off-axis angles. The rotated plywood structure is too complex to enable us to identify ''by inspection'' the responsible structural parameters. We do, however, note that in the model in which five sublamellae make up a lamellar unit (thick and thin lamellae with intervening transition zones) [11], the collagen orientations process at discrete 30° increments from 0 to 120° relative to the long axis of the bone. The fifth so-called ''back-flip'' sublamella is particularly prominent in these baboon bones (Fig. 2). This is therefore one possible structural parameter that could account for the observed differences in modulus values in different orientations. It would mostly affect the CLB specimens, where the lamellae are planar as compared to the osteonal bone. In the latter, the cylindrical organization of the lamellae minimizes this effect by having the off-axis features oriented in opposite directions on both sides of each cylinder (Fig. 10).

The baboon bones studied here showed a clear-cut dependence of flexural modulus values on specimen orientation. The anisotropy ratio (Table III) obtained (1.8) was almost identical to the highest values obtained by Reilly and Burstein [33] for the elastic properties in tension of human femurs, and was similar to other measurements using sonic velocity [36, 39, 40]. The absolute flexural modulus values of the CLB bones were higher at each orientation than the equivalent OB values. As both porosity and mineral content also affect modulus values [16], and as these are different in the CLB and OB specimens, a direct comparison of absolute values cannot be made. Currey [16] reported equations that relate both these parameters to the elastic modulus. Fig. 11 shows the results of calculations where we have used these equations to estimate the modulus values of CLB bones ''adjusted'' to have the same porosity and mineral content as measured in the OB bones (Table II). The recalculated CLB modulus values are lower than the measured values. The absolute extent of the shift towards lower values depends on the specific equations used and their inherent errors. As the direction of the shift is unlikely to change, this indicates that the lamellar structure in the form of osteons as opposed to planar arrays, probably contributed rather little to the absolute modulus values. These are mostly a function of the porosity, mineral content and particularly the lamellar structure itself. The latter is also variable. Polarized light microscopy shows that the proportions of mineralized collagen fibrils oriented in certain directions can differ between osteons or on the average between different sectors of the same bone [19–22]. The latter may be relevant to the measurements in this study, as we were obliged to obtain the CLB specimens from the medial side of the diaphysis, and the OB specimens from the lateral side.

The trends of the bending strength measurements of the CLB and OB specimens (Fig. 5) are similar to those observed for the flexural modulus. Bending strength was also affected by mineral content and porosity in much the same way as the modulus [38], and when these are taken into account, the two bone types were similar in this respect as well.

The calculated values of the ultimate properties of the CLB and OB specimens, fracture strain and nominal

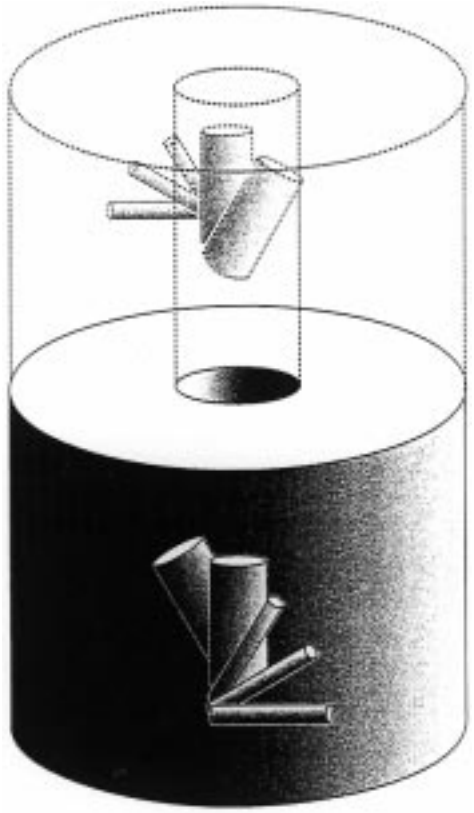

Figure 10 Schematic illustration of a single osteon showing the five sublamellae that make up a single lamellar unit [11] oriented in one direction on one side of the osteon and in the opposite direction on the other side. Following Fig. 2, both the fourth and fifth (''backflip'') sublamellae are particularly prominent in the baboon tibia.

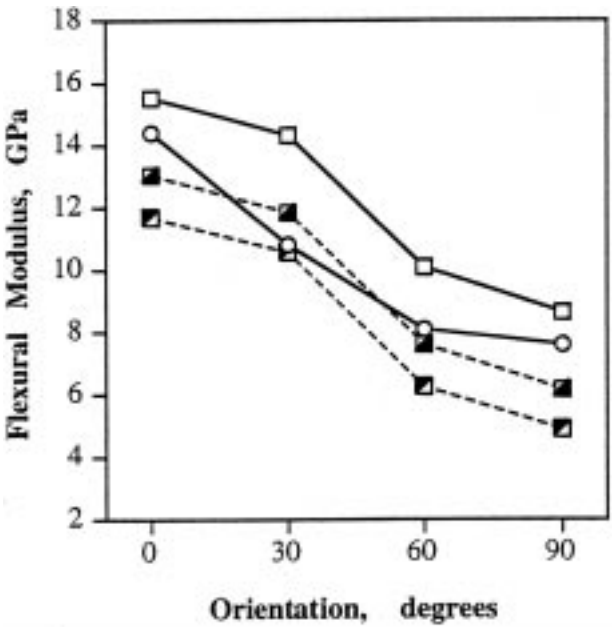

Figure 11 Graph showing the variations in the flexural modulus as a function of specimen orientation of the measured values (solid lines) for CLB specimens (—□—) and OB specimens (—○—) as shown in Fig. 4a. The dashed lines show the calculated values of hypothetical CLB specimens that have the same mineral content and porosity as the osteonal bone specimens. The calculations are based on Equations 9 and 10 in Currey [16] using either the linear form (- - -◪- - -) or power law (- - -◪- - -). The calculations were made for the 0° CLB specimens and then the same magnitude of offset was applied to the other orientations.

work-to-fracture, were similar both with respect to trends and absolute values. The only exceptional points were the 30° values for the nominal work-to-fracture, which are different. Disregarding this one difference, which is not understood at this point, this implies that the ultimate properties are also much influenced by the lamellar structure itself. Mineral content and porosity have a reciprocal relation to the work-to-fracture of bones [41]. It is therefore possible that as the CLB specimens had higher mineral contents and lower porosity than the OB specimens, these variables offset each other resulting in rather similar ultimate properties for both bone types.

One of the most remarkable observations, was the enormous dependence of both the fracture strain and the nominal work-to-fracture on sample orientation, with maximum anisotropy ratios of around 20 (Table III). Bearing in mind that it is the 0° orientation in which the force is applied perpendicular to the bone long axis, and that this is a frequent mode of fracture in nature, this property clearly has significant biological benefits. This anisotropy was still maintained even if the CLB samples were rotated around their long axes by 90° into the type B orientation, although the extent of anisotropy was less (Table III). The specific aspects of the lamellar structure responsible for this anisotropy in ultimate properties, are not known. Examination of the fracture surfaces does provide some insight.

At low magnification in the light and electron microscopes the CLB and OB 90° specimens were seen to have rather flat surfaces (Figs 6 and 7), oriented mostly in the *x–z* plane of the bone (Fig. 3). This is also the plane in which most of the stress is concentrated in the tension mode. In a sense, the material behaves in this orientation, more or less as a brittle solid. In contrast, the CLB and OB 0° specimens had undulating fracture surfaces (Figs 6 and 7), with one predominant direction in the *y–z* plane and the other in the *x–y* plane (Fig. 3). In this case it was the *y–z* plane in which most of the stress was concentrated in the tension mode. The tendency of the crack to also follow the *x–y* plane showed that this is a plane of structural weakness. SEM examination of this fracture surface showed that no specific plane is preferred, although the thick lamella surface is prominent (Fig. 12).

Figure 12 SEM micrograph of the fracture surface of a CLB specimen type A at 0° viewed in the *x–y* plane, *i.e.* parallel to the lamellar boundary planes (and the periosteal surface). Note that the plane does not follow one particular surface within a lamellar unit. Note too that several sets of differently aligned mineralized collagen fibril arrays can be seen. This view of the lamellar structure in the SEM is similar to the collagen fibril structural organization shown by Weiner *et al*. [11] using transmission electron microscopy for rat lamellar bone, where the fibril arrays are offset by roughly 30° increments.

Closer examination of these planes at higher magnification in the SEM revealed some interesting differences in both CLB and OB specimens. The *x–z* fracture plane on a 90° oriented specimen (Figs 7b and 7d and 2) consistently showed the lamellar structure, with an interesting ''saw-tooth'' pull-out structure along the lamellae. These are mainly clusters of mineralized collagen fibrils that make up the central portion (thick lamella) of a lamellar unit viewed in this direction. The fracture surfaces in the *y–z* plane showed no evidence of the lamellar structure, but have a ceramic-like texture (Fig. 7a and c). There was also an indication at high magnification of mineralized collagen fibrils causing a pull-out texture, but it was less pronounced than in the *x–z* plane. Most surprising, however, was the fact that the lamellar boundary planes were not evident, even though they do pass through this plane. This paradox is even more perplexing when it is taken into account that the proportions of collagen fibrils with different orientations in the *y–z* and *x–z* planes are rather similar (but not identical), when decalcified specimens are observed in the scanning and transmission electron microscopes [11, 13, 42]. The differences in fracture behavior may therefore be more related to varying crystal organizational structures in these two orthogonal planes. This structural anisotropy is also evident in the observed differences in the type A and B oriented CLB specimens. The bending strength, fracture strain and nominal work-to-fracture of type A specimens were generally higher than type B in the 0 and 30° orientations, but are similar for the 60 and 90° orientations. This is a fascinating subject for further structural investigation.

The CLB and OB specimens did, however, differ in two important respects, namely the extent to which the latter incur damage during fracture as compared to the former (Fig. 4), and the tendency of the two halves of the fractured osteonal bones to remain connected well after the main fracture event (Fig. 9). The possible biological significance of these observations of fracture behavior could be that even after fracture, the presence of the osteons significantly increases the chance of the fracture being successfully repaired, by minimizing the probably fatal consequences in nature of a non-union fracture. A similar behavior is seen in the ''greenstick'' fracture of children's bones. Both these features are presumably related in some way to the osteonal structure and the cement lines that surround each osteon. They may also be affected by the differences in mineral content and porosity. The cement line is known to promote crack arrest [27, 43] and crack propagation is inhibited by increased numbers of osteons [44]. Fracture studies of osteonal bone have reported pull-out features in which whole osteons are involved, pointing to the cement lines as surfaces of weakness [32, 45]. We did not observe such features in this study. The pull-out features we observed appeared to be localized bundles of aligned mineralized collagen fibrils.

Relating the structure of lamellar bone to its mechanical properties is a very challenging prospect,

that realistically can only be achieved by using a mathematical model that integrates the structure and the mechanics. A variety of such models have been published and these are generally stringently tested for their ability to reproduce experimental measurements of the elastic modulus of bone in different orientations (e.g. Katz and Meunier [46], Sasaki *et al*. [47], Wagner and Weiner [48], and Currey *et al*. [49]). One limitation has been that the data used apply to complex bone structures, such as osteonal and plexiform (fibrolamellar) bone, but the models are, as yet, generally unable to incorporate such structural complexity. This study provides a set of data on the mechanical properties of planar arrays of lamellar bone in four different orientations that significantly simplifies the problem. We stress, however, that much still remains to be learned about mineralized collagen fibril organization and the overall lamellar structure itself, and in particular about the aspects of the structure that contribute to the anisotropic elastic and especially remarkable fracture properties.

Acknowledgments

We thank Dr Gideon Rodan, *Merck, Sharpe and Dohme*, for the bone specimens and helpful comments. We also thank Professor Lia Addadi for her helpful comments. This study was supported by a US Public Service grant (DEO6954) from the National Institute of Dental and Craniofacial Research, and in part by *Merck, Sharpe and Dohme*. S.W. holds the I.W. Abel Professorial Chair of Structural Biology.

References

1. J. D. CURREY, in ''The Mechanical Adaptations of Bones'' (Princeton University Press, Princeton, NJ, 1984).
2. D. H. ENLOW, *Texas J. Sci.* **10** (1958) 187.
3. A. DE RICQLÈS, F. J. MEUNIER, J. CASTANET and H. FRANCILLON-VIEILLOT, in ''Bone'', Vol. 3, edited by B. K. Hall (CRC Press, Boca Raton, FL, 1991) p. 1.
4. R. A. ROBINSON, *J. Bone Joint Surg.* **34A** (1952) 389.
5. M. J. GLIMCHER, *Rev. Mod. Phys.* **31** (1959) 313.
6. S. WEINER and W. TRAUB, *FEBS Lett.* **206** (1986) 262.
7. *Idem.*, *FASEB J.* **6** (1992) 879.
8. W. GEBHARDT, *Arch. Entwickl. Mech. Org.* **20** (1906) 187.
9. J. W. SMITH, *J. Anat.* **94** (1960) 329.
10. M. M. GIRAUD-GUILLE, *Calcif. Tissue Int.* **42** (1988) 167.
11. S. WEINER, T. ARAD, I. SABANAY and W. TRAUB, *Bone* **20** (1997) 509.
12. E. B. RUTH, *Amer. J. Anat.* **80** (1947) 35.
13. G. MAROTTI, *Calcif. Tissue Int.* **53** (1993) 547.
14. R. A. ROBINSON and S. R. ELLIOT, *J. Bone Joint Surg.* **39A** (1957) 167.
15. E. P. KATZ and S. LI, *J. Mol. Biol.* **80** (1973) 1.
16. J. D. CURREY, *J. Biomech.* **21** (1988) 131.
17. R. B. MARTIN and D. L. BOARDMAN, *ibid.* **26** (1993) 1047.
18. J. JOWSEY, *Clin. Orthop.* **17** (1960) 210.
19. F. G. EVANS and R. VINCENTELLI, *J. Biomech.* **2** (1969) 63.
20. C. M. RIGGS, L. C. VAUGHAN, G. P. EVANS, L. E. LANYON and A. BOYDE, *Anat. Embryol.* **187** (1993) 239.
21. M. W. MASON, J. G. SKEDROS and R. D. BLOEBAUM, *Bone* **17** (1995) 229.
22. R. B. MARTIN, S. T. LAU, P. V. MATHEWS, V. A. GIVSON and S. M. STOVER, *J. Biomech.* **29** (1996) 1515.
23. A. SIMKIN and G. ROBIN, *J. Biomech.* **6** (1973) 31.
24. A. ASCENZI, P. BASCHEIRI and A. BENVENUTI, *ibid.* **23** (1990) 763.
25. V. ZIV, H. D. WAGNER and S. WEINER, *Bone* **18** (1996) 417.
26. J. D. CURREY, *J. Anat.* **98** (1959) 87.
27. D. B. BURR, M. B. SCHAFFLER and R. G. FREDRICKSON, *J. Biomech.* **21** (1988) 939.
28. D. D. THOMPSON, J. G. SEEDOR, H. QUARTUCCIO, H. SOLOMON, C. FIORAVANTI, J. DAVIDSON, H. KLEIN, R. JACKSON, J. CLAIR, D. FRANKENFIELD, E. BROWN, H. A. SIMMONS and G. A. RODAN, *J. Bone Min. Res.* **7** (1992) 951.
29. R. BALENA, B. C. TOOLAN, M. SHEA, A. MARKATOS, E. R. MYERS, S. C. LEE, E. E. OPAS, J. G. SEEDOR, H. KLEIN, D. FRANKENFIELD, H. QUARTUCCIO, C. FIORAVANTI, J. CLAIR, E. BROWN, W. C. HAYES and G. A. RODAN, *J. Clin. Invest.* **92** (1993) 2577.
30. A. H. BURSTEIN, J. D. CURREY, V. H. FRANKEL and D. T. REILLY, *J. Biomech.* **5** (1972) 35.
31. T. S. KELLER, Z. MAO and D. M. SPENGLER, *J. Orthop. Res.* **8** (1990) 592.
32. D. D. MOYLE and R. W. BOWDEN, *J. Biomech.* **17** (1984) 203.
33. D. T. REILLY and A. H. BURSTEIN, *ibid.* **8** (1975) 393.
34. R. F. KER and P. ZIOUPOS, *Comments Theor. Biol.* **4** (1997) 151.
35. W. T. DEMPSTER and R. T. LIDDICOAT, *Amer. J. Anat.* **91** (1952) 331.
36. W. BONFIELD and M. D. GRYNPAS, *Nature* **270** (1977) 453.
37. J. L. KATZ, *ibid.* **283** (1980) 106.
38. J. D. CURREY, *Phil. Trans. R. Soc. Lond. B* **304** (1984) 509.
39. C. H. TURNER, A. CHARDRAN and R. M. V. PIDAPARTI, *Bone* **17** (1995) 85.
40. J. L. KATZ, H. S. YOON, S. LIPSOM, R. MAHARIDGE, A. MEUNIER and P. CHRISTEL, *Calcif. Tissue Int.* **36** (1984) S31.
41. *Idem.*, *J. Biomech.* **23** (1990) 837.
42. V. ZIV, I. SABANAY, T. ARAD, W. TRAUB and S. WEINER, *Microsc. Res. Tech.* **33** (1996) 203.
43. J. D. CURREY, *Quart. J. Microscope Sci.* **103** (1962) 111.
44. G. CORONDAN and W. L. HAWORTH, *J. Biomech.* **19** (1986) 207.
45. K. PIEKARSKI, *J. Applied. Phys.* **41** (1970) 215.
46. J. L. KATZ and A. A. MEUNIER, *J. Mater. Sci. Mater. Med.* **1** (1990) 1.
47. N. SASAKI, T. IKAWA and A. FUKUDA, *J. Biomech.* **24** (1991) 57.
48. H. D. WAGNER and S. WEINER, *ibid.* **25** (1992) 1311.
49. J. D. CURREY, K. BREAR and P. ZIOUPOS, *ibid.* **27** (1994) 885.

Received 20 February
and accepted 31 August 1998